

## S1 Detailed WRF configuration

Table S1 contains information on the configuration of the model as used in the experiment.

Basic information				
Domain codes		d01	d02	d03
Resolution		10 km x 10 km	2 km x 2 km	0.4 km x 0.4 km
Vertical resolution		85 full-model levels		
Model top		50 hPa, approximately 20 km a.m.s.l.		
Levels below 3 km a.g.l.		38		
Time step		50 s	10 s	2 s
Feedback option		off		
Parameterizations				
Microphysics		Thompson et al. (2004)		
Longwave radiation		RRTMG (Iacono et al., 2008)		
Shortwave radiation		RRTMG (Iacono et al., 2008)		
Surface layer		Revised MM5 (Jiménez et al., 2012)		
Land surface model		Noah LSM (Chen and Dudhia, 2001)		
Cumulus parameterization	GD (Grell and Dévényi, 2002)		off	off
PBL scheme		Shin and Hong (2015)		
Land use maps		MODIS 30" with lakes		
Elevation		GMTED 30"		
Nudging				
On/off		on, to ECMWF HRES	off	off
Variables		wind, T, q <sup>a</sup>		
Interval		180 min		
Wind nudging levels		all levels		
Wind nudging coeff.		$3.0 \times 10^{-4} \text{ s}^{-1}$		
T nudging levels		$\geq 40$ (above 3 km)		
T nudging coeff.		$3.0 \times 10^{-4} \text{ s}^{-1}$		
q nudging levels		$\geq 40$ (above 3 km)		
q nudging coeff.		$4.5 \times 10^{-5} \text{ s}^{-1}$		

<sup>a</sup> - Here q denotes water vapour mixing ratio, defined as kg of vapour per kg of dry air, in accordance with WRF naming convention.

**Table S1.** Details of WRF-GHG model configuration.

## S2 Emissions and mole fractions at emission point

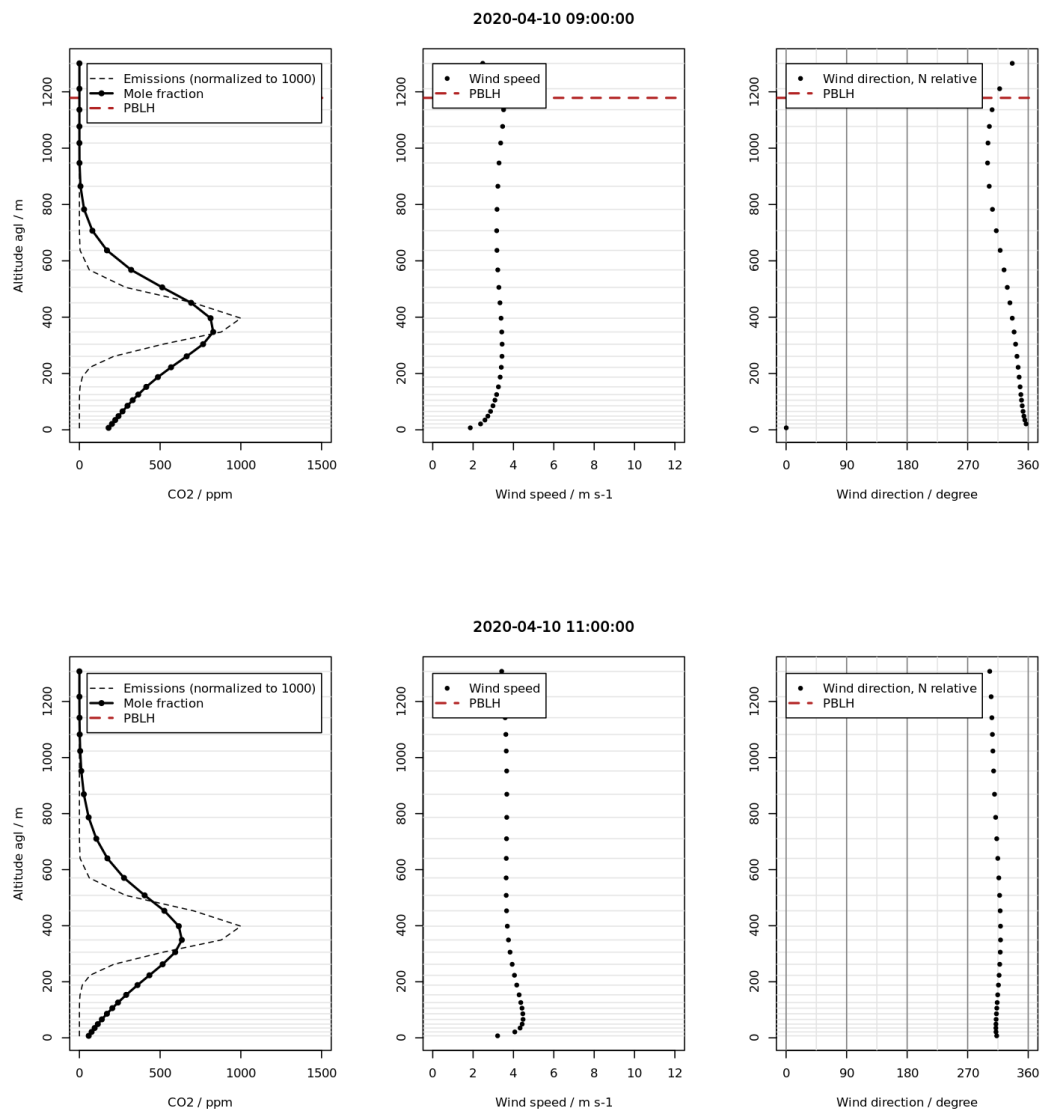


**Figure S1.** Vertical profiles of selected model variables at the emission point (Bełchatów Power Plant). Top: data from 09:00 UTC, 10 April 2020, extracted from WRF 400 m x 400 m output. Bottom: Same for 11:00 UTC. Left: CO<sub>2</sub> mole fractions in ppm (solid line). Vertical distribution of CO<sub>2</sub> emissions, normalized to 1000 (arbitrary units; dashed). Centre: wind speed (points) and Planetary Boundary Layer Height (PBLH, red, dashed). Right: wind direction and PBLH.

### S3 Dry-air mole fractions of CO<sub>2</sub> tagged tracers (puffs)

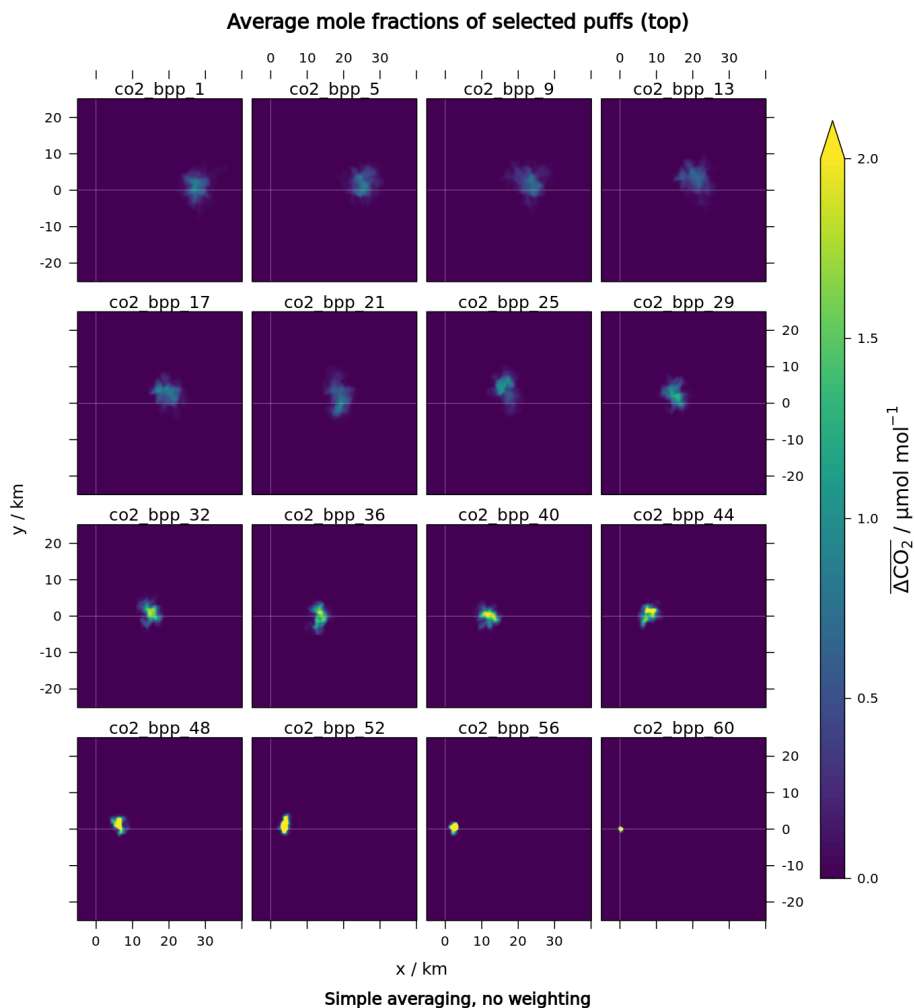


**Figure S2.** Average mole fraction of the temporally-tagged CO<sub>2</sub> tracers (puffs) at 12:00 UTC. Simple vertical averaging of mole fractions are presented. Effects of the gradual dispersion of the plume emitted at the power plant (located at  $x = 0$ ,  $y = 0$ ) is visible, with old tracers (e.g. co2\_bpp\_1 emitted between 09:00 – 09:03 UTC) spreading spatially as they move along the mean wind direction (increasing  $x$ ). The final tracer, co2\_pbb\_60 was emitted between 11:57 – 12:00 UTC and the emitted mass is still in the direct vicinity of the source.

## 5 S4 Tracer mass discrepancies in the analysis area

In order to test whether the sum of individual tagged tracers (i.e. puffs) can be used to quantitatively interpret the emitted CO<sub>2</sub> plume, we have compared column-integrated values of the sum of puffs to a classical, reference tracer. As can be seen in Fig. S4, for the analysis area discussed in the study, namely 2–22 km range, local discrepancies caused by high local gradients occur only in the immediate vicinity of the emission source and are affecting the mass distribution locally at distances lower than 5 km. However, the total mass of the emitted plume is well preserved in both cases, with two versions of the plume carrying mass identical within 0.035 %.

We conclude that for the purposes of this study, both tracers can be treated as identical.

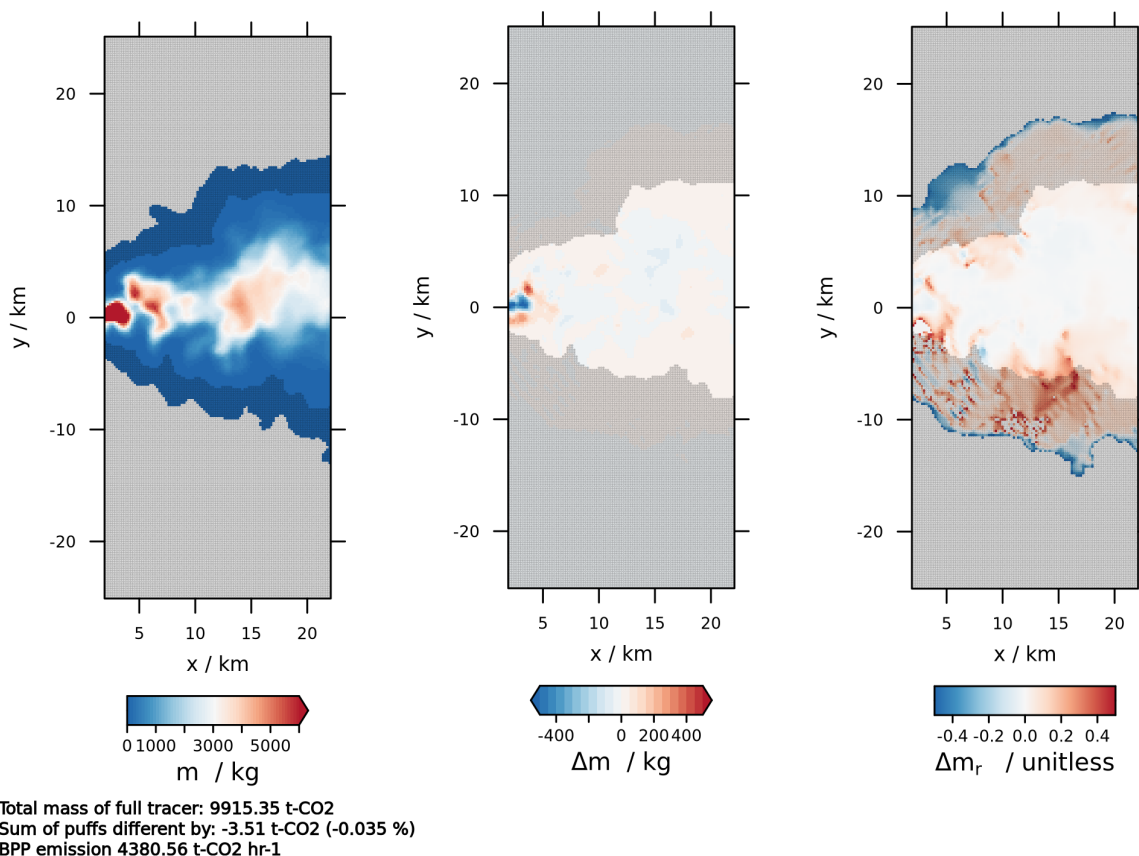


**Figure S3.** Left: Total column integrated mass of CO<sub>2</sub>. Middle: mass discrepancy in the analysis area (2–22 km between the sum of 60 temporally-tagged tracers (co2\_bpp\_1 to co2\_bpp\_60) and the full tracer signal (reference) caused by the model’s mass-conserving advection scheme. Right: relative pointwise mass discrepancy ( $\Delta m/m$ ). Relative mass discrepancy integrated over the area shown is 0.35 ‰. Shaded areas in the figure panels contain  $10^{-4}$  of the total tracer mass in the presented spatial extent.

## References

- 15 Chen, F. and Dudhia, J.: Coupling an Advanced Land Surface–Hydrology Model with the Penn State–NCAR MM5 Modeling System. Part I: Model Implementation and Sensitivity, *Monthly Weather Review*, 129, 569 – 585, [https://doi.org/10.1175/1520-0493\(2001\)129<0569:CAALSH>2.0.CO;2](https://doi.org/10.1175/1520-0493(2001)129<0569:CAALSH>2.0.CO;2), 2001.
- Grell, G. A. and Dévényi, D.: A generalized approach to parameterizing convection combining ensemble and data assimilation techniques, *Geophysical Research Letters*, 29, 38–1–38–4, <https://doi.org/https://doi.org/10.1029/2002GL015311>, 2002.
- 20 Iacono, M. J., Delamere, J. S., Mlawer, E. J., Shephard, M. W., Clough, S. A., and Collins, W. D.: Radiative forcing by long-lived greenhouse gases: Calculations with the AER radiative transfer models, *Journal of Geophysical Research: Atmospheres*, 113, <https://doi.org/https://doi.org/10.1029/2008JD009944>, 2008.
- Jiménez, P. A., Dudhia, J., González-Rouco, J. F., Navarro, J., Montávez, J. P., and García-Bustamante, E.: A Revised Scheme for the WRF Surface Layer Formulation, *Monthly Weather Review*, 140, 898 – 918, <https://doi.org/10.1175/MWR-D-11-00056.1>, 2012.
- 25 Shin, H. H. and Hong, S.-Y.: Representation of the Subgrid-Scale Turbulent Transport in Convective Boundary Layers at Gray-Zone Resolutions, *Monthly Weather Review*, 143, 250 – 271, <https://doi.org/10.1175/MWR-D-14-00116.1>, 2015.
- Thompson, G., Rasmussen, R. M., and Manning, K.: Explicit Forecasts of Winter Precipitation Using an Improved Bulk Microphysics Scheme. Part I: Description and Sensitivity Analysis, *Monthly Weather Review*, 132, 519 – 542, [https://doi.org/10.1175/1520-0493\(2004\)132<0519:EFOWPU>2.0.CO;2](https://doi.org/10.1175/1520-0493(2004)132<0519:EFOWPU>2.0.CO;2), 2004.